Short Communication

On-line monitoring of lead–acid batteries by galvanostatic non-destructive technique

B. Hariprakash [a], S.K. Martha [a], Arthi Jaikumar [a], A.K. Shukla [a,b,*]

[a] Solid State and Structural Chemistry Unit, Indian Institute of Science, Bangalore 560012, India
[b] Central Electrochemical Research Institute, Karaikudi 623006, India

Abstract

Measurements of charge-acceptance, internal resistance, voltage and self-discharge of a battery reflect its state-of-health (SOH). The galvanostatic non-destructive technique (GNDT) can be used to monitor the SOH of a battery by analyzing its impedance parameters, namely ohmic resistance, charge-transfer resistance and interfacial capacitance. In this technique, the battery is discharged galvanostatically at a substantially low-rate over a short duration, wherein the state-of-charge (SOC) of the battery is not affected. It has been possible to obtain charge-transfer resistance and double-layer capacitance values for both positive and negative plates of a commercial grade 6-V/4-Ah valve-regulated lead–acid battery during its dynamic discharge. The resistive components of the battery are found to be minimum at state-of-charge values between 0.2 and 0.9. The study shows that the optimum performance of the VRLA battery can be achieved at SOC values between 0.2 and 0.9. The ohmic resistance of the battery displays a linear variation with logarithmic values of its SOC. The technique provides an attractive tool for on-line monitoring of lead–acid batteries.
© 2004 Elsevier B.V. All rights reserved.

1. Introduction

The state-of-charge (SOC) of a battery is reflected by the electrical response associated with the battery's resistance where the application of a load causes the battery voltage to drop instantaneously. This phenomenon has been targeted by researchers for determining the resistance and, therefore, is as an indicator of the discharged capacity of the battery. Since the open-circuit voltage of a battery is a fixed quantity and its discharge circuit is also not altered, it is quite obvious that the internal resistance of the battery will increase with its depth-of-discharge along with its voltage on-charge. Accordingly, if the discharge behaviour of the battery is known a priori then its state-of-health (SOH) can be easily estimated. It is noteworthy that with ageing of the battery, the discharge capacity of the battery decreases owing to an increase in its internal resistance. Accordingly, the SOH of any sealed battery can be predicted from a knowledge of its internal resistance [1].

At present, lead–acid is the most ubiquitous battery in the global rechargeable battery market and, in terms of value,

present world sales are about US$ 10 billion per annum [2]. The on-going electrification of automobiles makes a reliable diagnostic necessary for the vehicle's energy-storage units. Since valve-regulated lead–acid (VRLA) batteries are expected to become important energy-storage technology for near-term vehicles, monitoring and diagnostic algorithms for these batteries are of great importance. Besides, with the introduction of 36-V/42-V Powernets and the increase of electrically-assisted features, e.g., idle-stop operation and launch assistance, the importance of a suitable battery monitoring and management will increase even further. It has been reported [3–33] that several methods are being employed to monitor the SOH of various battery systems. As a part of our ongoing research programme on battery monitoring [6–9], we describe on-line monitoring of lead–acid batteries by a galvanostatic non-destructive technique (GNDT) [34].

2. Experimental

A 6-V/4-Ah commercial grade VRLA battery was formed by galvanostaic charge-discharge cycling. During formation cycles, the battery was charged and discharged at the C/10 and the C/5 rate, respectively. Subsequent to formation, the

* Corresponding author. Tel.: +91 80 22932795; fax: +91 80 23601310.
E-mail address: shukla@sscu.iisc.ernet.in (A.K. Shukla).

GNDT was used to characterize, the battery at different SOC values. The SOC value of the battery was taken as unity in its fully-charged state and zero when the battery voltage was 1.75 V. The technique involves discharge of the test cell at a substantially low-rate, namely C/150, over a period of only about 50 s. The data were collected at intervals of 10 ms over a total duration of 50 s using an AUTOLAB PGSTAT30 (EcoChemie, Utrecht, The Netherlands). All experiments were performed at 25(±1) °C. The data were fitted and analyzed with the aid of Microcal Origin software. Both the data-collection and analysis were repeated at several SOC values of the test battery in order to ensure reproducibility.

3. Galvanostatic non-destructive technique

GNDT is a technique to monitor the SOH of a battery by analyzing its impedance parameters [34]. Since the discharge current corresponding to the C/150 rate is restricted to a duration of 50 s only, the SOC of the test battery can be taken to be nearly invariant for all practical purposes. Accordingly, it can be assumed that the charge-transfer processes are the rate-determining steps for both the electrode reactions. Since the electrode processes are not governed by mass transfer, the Warburg components are not included in the equivalent circuit [34,35]. Accordingly, the equivalent circuit of the test cell under GNDT conditions is shown in Fig. 1, where T_1 and T_2 are the cell terminals, R_Ω is the ohmic resistance, $R_{t,1}$ and $C_{d,1}$ are the charge-transfer resistance and the interfacial capacitance, which includes the double-layer capacitance and associated capacitive components due to adsorption, passive films, etc., for one of the electrodes, while $R_{t,2}$ and $C_{d,2}$ are the charge-transfer resistance and the interfacial capacitance for the other electrode.

Under GNDT conditions, the overpotentials are mainly due to charge-transfer polarization at the two electrodes in their respective linear polarization domain. Following the convention chosen for the current due to an electrode reaction (namely, cathodic current as positive), it follows that $\eta_1 > 0$ and $\eta_2 < 0$ during discharge of the battery, where η_1 and η_2 refer to the overpotential at the anode and the cathode, respectively. Accordingly, from Kirchoff's voltage law:
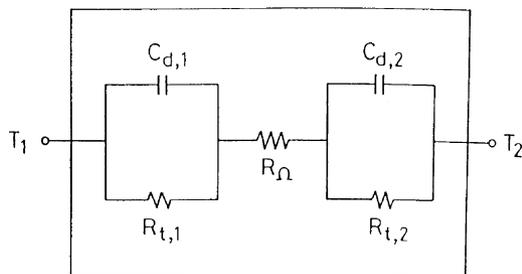

Fig. 1. Equivalent circuit for test battery under GNDT conditions.

$$V^r - V - \eta_1 - IR_\Omega + \eta_2 = 0 \tag{1}$$

$$V^r - V = \eta_1 - \eta_2 + IR_\Omega \tag{2}$$

where V^r is the equilibrium voltage of the test cell; V is the voltage of the cell during galvanostatic discharge; IR_Ω is the ohmic resistance of the cell.

When there is a change in galvanostatic discharge current at time x, for a short duration of y seconds, Eq. (2) becomes:

$$V^x - V = \eta_1' - \eta_2' + IR_\Omega \tag{3}$$

where V^x is the voltage of the cell at time x.

In order to eliminate η_1' and η_2' in Eq. (3) and express them in terms of the appropriate impedance parameters, Kirchoff's law may be applied to the two junctions of R_Ω with the $R_{t,1}$–$C_{d,1}$ and $R_{t,2}$–$C_{d,2}$ branches, as shown in Fig. 1. According to the sign convention adopted for the anodic (I_a) and cathodic (I_c) currents, we have,

$$-I_a = -C_{d,1}\left(\frac{d\eta_1'}{dt}\right) - \left(\frac{\eta_1'}{R_{t,1}}\right) \tag{4}$$

and,

$$I_c = -C_{d,2}\left(\frac{d\eta_2'}{dt}\right) - \left(\frac{\eta_2'}{R_{t,2}}\right) \tag{5}$$

Integrating Eq. (4) and solving for η_1' gives:

$$-\eta_1' = -IR_{t,1} + K_1 \exp\left(\frac{-t}{\tau_1'}\right) \tag{6}$$

where $\tau_1' = R_{t,1} \cdot C_{d,1}$

At time $t = x^+$, i.e., immediately after change in galvanostatic current where $\eta_1' = 0$, $K_1 = IR_{t,1}$, Eq. (6) yields,

$$\eta_1' = IR_{t,1}\left[1 - \exp\left(\frac{-t}{\tau_1'}\right)\right] \tag{7}$$

Similarly,

$$-\eta_2' = IR_{t,2}\left[1 - \exp\left(\frac{-t}{\tau_2'}\right)\right] \tag{8}$$

Substituting Eqs. (7) and (8) in Eq. (3) yields:

$$V^x - V = IR_\Omega + IR_{t,1}\left[1 - \exp\left(\frac{-t}{\tau_1'}\right)\right] + IR_{t,2}\left[1 - \exp\left(\frac{-t}{\tau_2'}\right)\right] \tag{9}$$

For a small current perturbation, the voltage response of the test battery can be written as Eq. (9) with reference to the equivalent circuit shown in Fig. 1, where V^x is the voltage of the cell at time x, V is the voltage of the cell at a particular time, I is the discharge current, and τ_1 ($= R_{t,1}C_{d,1}$) and τ_2 ($= R_{t,2}C_{d,2}$) are the time constants of the associated electrode processes. The exponential terms in Eq. (9) are due to charging of the electrical double-layers at the constituent plates of the lead–acid battery with respective double-layer capacitance values of $C_{d,1}$ and $C_{d,2}$. At time $t > \tau_1$ and
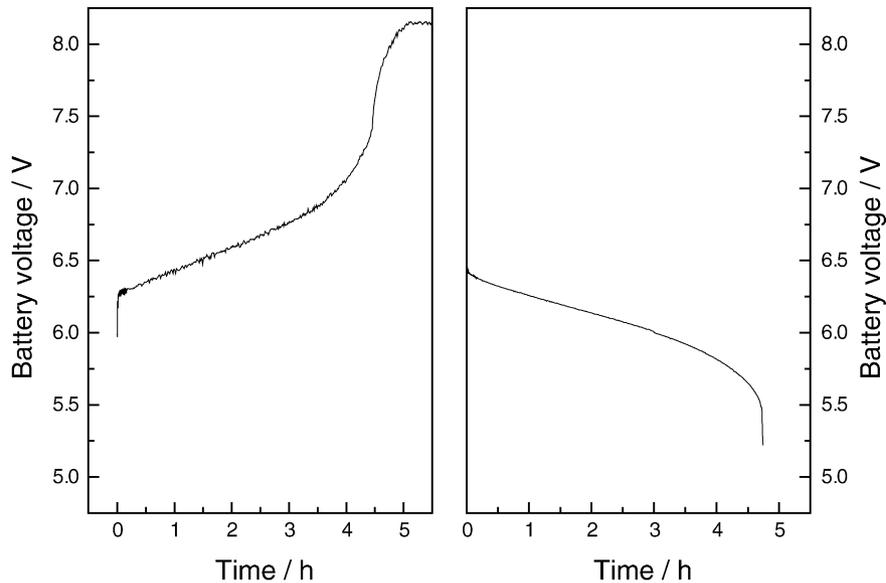
Fig. 2. Typical charge–discharge curves at C/5 rate and 25 °C for 6-V/4-Ah lead–acid battery.

τ_2, the capacitors are completely charged and therefore the voltage drop is only due to resistive components [34,35], namely $R_{t,1}$, $R_{t,2}$ and R_Ω.

A solution of Eq. (9) provides the impedance parameters of the cell. Since there are serious limitations in the direct algebraic procedure to solve Eq. (9), an alternative approach is adapted by considering the time constants, namely τ_1 and τ_2, to differ by an order of magnitude. The detailed procedure is explained elsewhere [6–9].

4. Results and discussion

The lead–acid battery was found to attain its maximum capacity within three charge-discharge cycles. Typical charge–discharge curves at 25 °C at the C/5 rate are shown in Fig. 2. The battery yields a Faradaic efficiency of about 90%. A typical battery resistance transient at SOC = 0.9 for 50 s is shown in Fig. 3. The voltage response is exponential in accordance with Eq. (9) and the data are fitted using a Microcal Origin algorithm. The fit for the data shown in Fig. 3 is given in the inset from which the impedance data are obtained for the test battery at a particular SOC value, where $y(0)$ corresponds to the ohmic resistance of the battery, $A(1)$ and $A(2)$ are the charge-transfer resistances, and $t(1)$ and $t(2)$ are the time constants for the constituent plates.

The ohmic resistance for the battery at varying states-of-charge is presented in Fig. 4. The values increase monotonically with decrease in SOC, and this is due to a decrease in the active-material conductivity as it becomes converted from PbO_2 and Pb at positive and negative plates, respec-
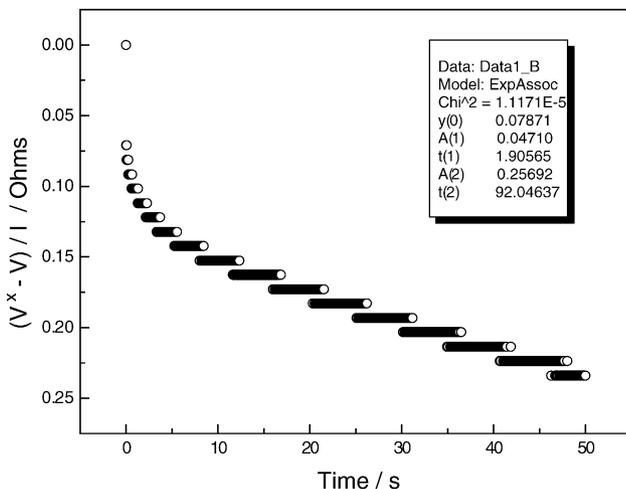

Fig. 3. A typical lead–acid battery resistance transient at SOC = 0.9.
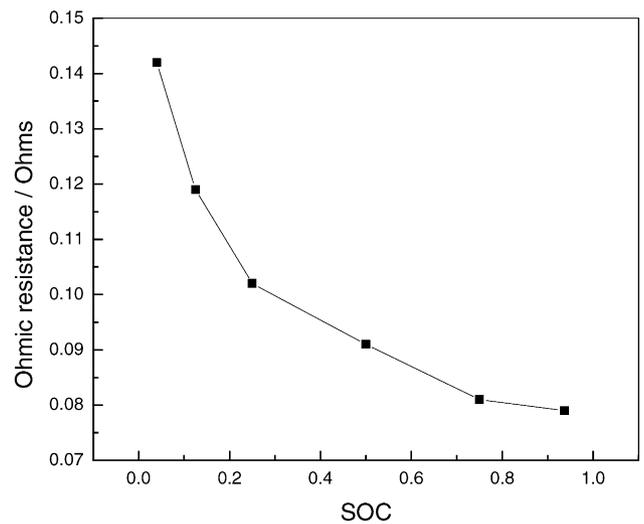

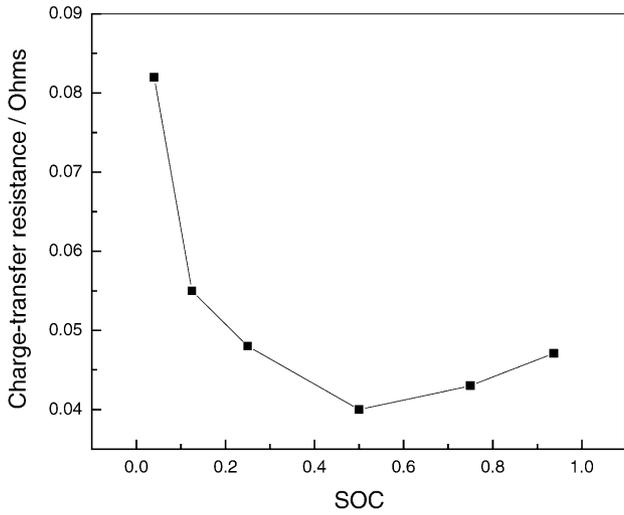Fig. 4. Ohmic resistance values as function of SOC for 6-V/4-Ah lead–acid battery.

Fig. 5. Charge-transfer resistance values as function of SOC for $Pb|PbSO_4$ electrode of 6-V/4-Ah lead–acid battery.
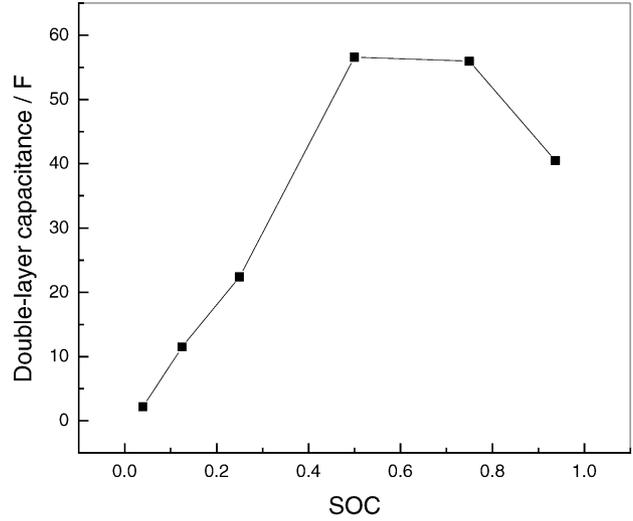

Fig. 6. Charge-transfer resistance values as a function of SOC for $PbO_2|PbSO_4$ electrode of 6-V/4-Ah lead–acid battery.

Fig. 7. Total internal resistance values as function of SOC for 6-V/4-Ah lead–acid battery.

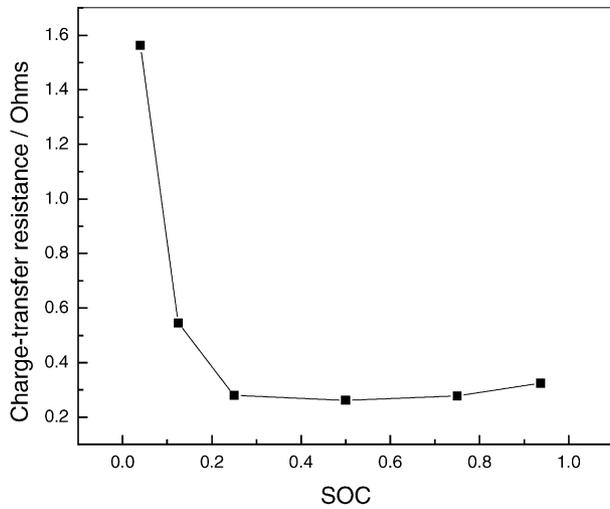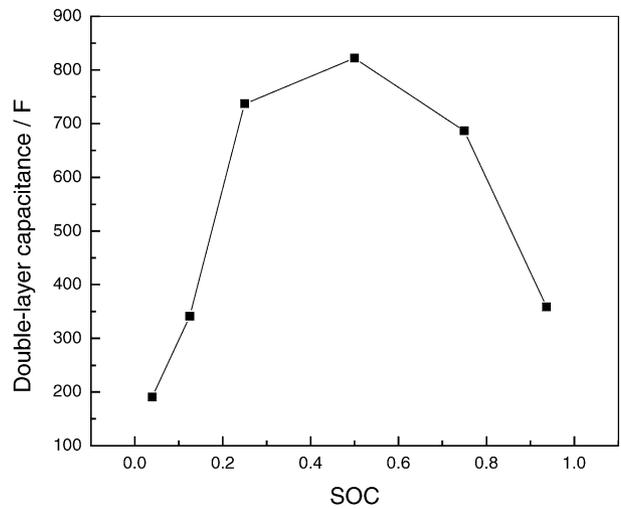Fig. 8. Double-layer capacitance values as function of SOC for $Pb|PbSO_4$ electrode of 6-V/4-Ah lead–acid battery.

Fig. 9. Double-layer capacitance values as function of SOC for $PbO_2|PbSO_4$ electrode of 6-V/4-Ah lead–acid battery.
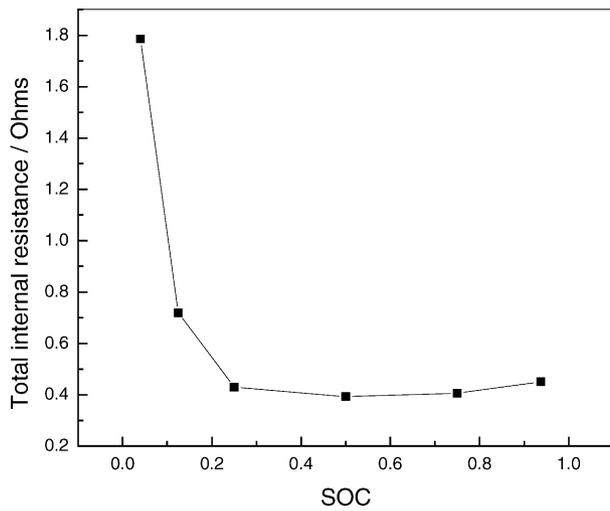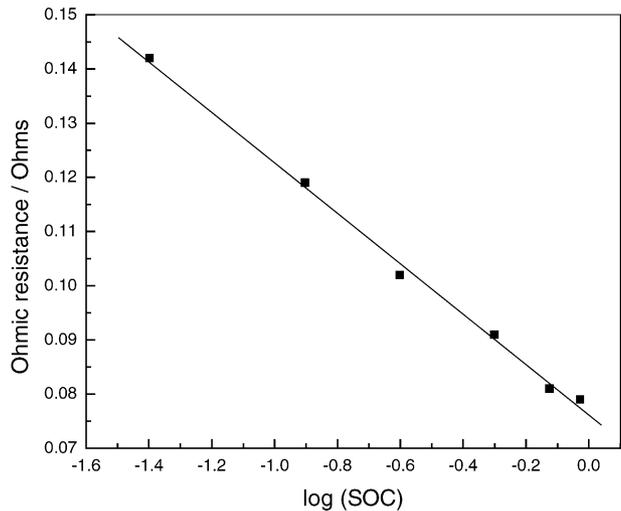

Fig. 10. Ohmic resistance values as function of log (SOC) for 6-V/4-Ah lead–acid battery.
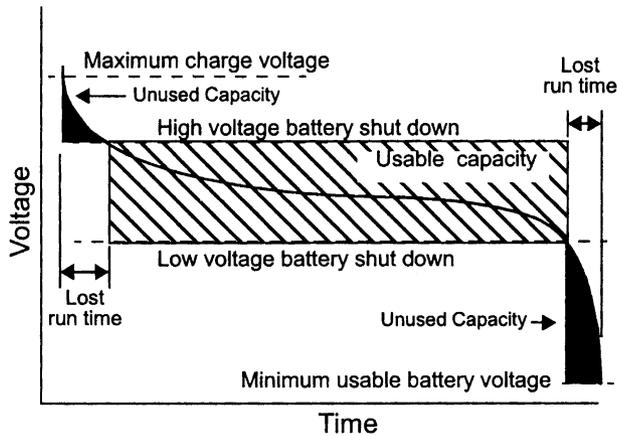
Fig. 11. Effective capacity window of battery.

tively, to $PbSO_4$. The charge-transfer resistance values for the negative electrode as a function of its SOC are given in Fig. 5. The increased charge-transfer resistance values obtained near SOC = 1 could be due to a gas layer on the electrode surface. The charge-transfer resistance values decrease towards SOC = 0.5 from SOC = 1, and increase towards SOC = 0 from SOC = 0.5. The variation in the charge-transfer resistance values as a function of SOC for the positive plate is shown in Fig. 6. There is gradual increase in charge-transfer resistance values towards SOC = 0.2, and the change in charge-transfer resistance is drastic towards SOC = 0 from SOC = 0.2, which suggests that the battery is limited by the positive plate. Also, the charge-transfer resistance values of the positive plate are considerably higher than those for the negative plate. This is because lead is a better electrical conductor than PbO_2. In both the plates, the increase in charge-transfer resistance values towards SOC = 0 is due to the conversion of both Pb and PbO_2 to poorly

conducting $PbSO_4$. The total internal resistance values as a function of SOC are shown in Fig. 7.

The double-layer capacitance for the Pb and PbO_2 plates are presented in Figs. 8 and 9, respectively. The values for the positive plates are higher by an order magnitude than those for the negative plates. It is clear that the plates can deliver high power at SOC values in between 0.9 and 0.2. Also, from total internal resistance values, it is clear that the cycle-life of the battery could be improved when it is operated at SOC values between 0.9 and 0.2.

It is noteworthy that the ohmic resistance of the battery shows a linear variation with logarithmic values of its SOC, which provides an attractive tool for online monitoring of lead–acid batteries as shown in Fig. 10. The effective capacity window of a battery is shown in Fig. 11 [36]. This technique supports monitoring batteries effectively in this window. Ohmic resistance values as a function of SOC at different cycles for the battery are also shown in Fig. 12, from which the ageing parameter can be easily predicted.

5. Conclusions

The data from the present study indicate that a marked variation in the internal resistance of the VRLA battery occurs in the SOC values between 0 and 0.2 as well as between 0.9 and 1.0. This suggests that the operation of the battery in this range of SOC values may lead to deleterious effects. The charge-transfer resistance values of the positive ($R_{t,2}$) and negative ($R_{t,1}$) plates of the VRLA battery under examination are found to be minimum over the SOC range between 0.2 and 0.9. It would be therefore preferable to limit the operation of VRLA batteries in this SOC range. Since, $R_{t,1}$ is lower than $R_{t,2}$, it is suggested that the perfor-
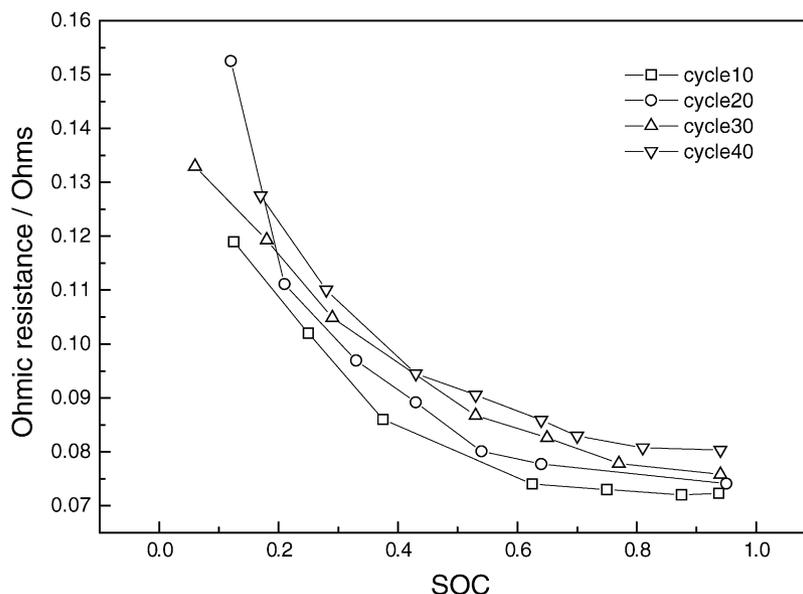

Fig. 12. Ohmic resistance values as function of SOC for 6-V/4-Ah lead–acid battery at increasing cycle-life.

mance of the VRLA battery employed in this study can be improved by electrocatalysis of the $PbO_2/PbSO_4$ reaction. Variation in the interfacial capacitance of both positive and negative plates with SOC values has also been monitored. It has been found that the ohmic resistance of the battery shows a linear variation with logarithmic values of its SOC, which offers an attractive means for the on-line monitoring of lead–acid batteries.

References

[1] S. Buller, J. Walter, E. Karden, R.W. De Doncker, Advanced Automotive Battery Conference, Las Vegas, 2002.

[2] R.M. Dell, D.A. J. Rand, Understanding Batteries, Royal Society of Chemistry, UK, 2002.

[3] F. Fuet, J. Power Sources 70 (1998) 59.

[4] S. Piller, M. Perrin, A. Jossen, J. Power Sources 96 (2001) 113.

[5] S. Rodrigues, N. Munichandraiah, A.K. Shukla, J. Power Sources 87 (2000) 12.

[6] A.K. Shukla, V. Ganesh Kumar, N. Munichandraiah, T. Srinath, J. Power Sources 74 (1998) 234.

[7] V. Ganesh Kumar, N. Munichandraiah, A.K. Shukla, J. Appl. Electrochem. 27 (1997) 43.

[8] V. Ganesh Kumar, N. Munichandraiah, A.K. Shukla, J. Power Sources 63 (1996) 203.

[9] B. Hariprakash, S.K. Martha, A.K. Shukla, J. Power Sources 117 (2003) 242.

[10] K. Champlin, K. Bertness, in: Proceedings of the 22nd International Telecommunications Energy Conference, 2000, p. 348.

[11] J.M. Charlesworth, Electrochimi. Acta 41 (1996) 1721.

[12] S.R. Nelatury, P. Singh, J. Power Sources 112 (2002) 621.

[13] A.J. Salkind, C. Fennie, P. Singh, T. Atwater, D.E. Reisner, J. Power Sources 80 (1999) 293.

[14] Z. Stoynov, T. Nishev, V. Vacheva, N. Stamenova, J. Power Sources 64 (1997) 189.

[15] S. Martinet, R. Durand, P. Ozil, P. Lablanc, P. Blanchard, J. Power Sources 83 (1999) 93.

[16] D.O. Feder, M.J. Hlavac, S.J. McShane, J. Power Sources 48 (1994) 135.

[17] C. Armenta, J. Doria, M.C. De Andres, J. Urratia, J. Fullea, F. Grafia, J. Power Sources 27 (1989) 189.

[18] D.H.J. Baert, A.A.K. Vervaet, J. Power Sources 114 (2003) 357.

[19] P.J. Blood, S. Sotiropoulos, J. Power Sources 110 (2002) 96.

[20] V. Mancier, A. Metrot, P. Willmann, J. Power Sources 117 (2003) 223.

[21] V. Mancier, A. Metrot, P. Willmann, Electrochim. Acta 47 (2002) 1633.

[22] I.R. Hill, Ed.E. Andrukaitis, J. Power Sources 103 (2001) 98.

[23] P. Mauracher, E. Karden, J. Power Sources 67 (1997) 69.

[24] A. Jossen, V. Spath, H. Doring, J. Garche, J. Power Sources 84 (1999) 283.

[25] Z. Stoynov, B. Savova-stoynov, T. Kossev, J. Power Sources 30 (1990) 275.

[26] A. Salkind, T. Atwater, P. Singh, S. Nelatury, S. Damodar Jr., C. Fennie, D. Reisner, J. Power Sources 96 (2001) 151.

[27] A. Tenno, R. Tenno, T. Suntio, J. Power Sources 103 (2001) 42.

[28] E. Meissner, G. Richter, J. Power Sources 116 (2003) 79.

[29] E. Karden, S. Buller, R.W. De Doncker, Electrochim. Acta 47 (2002) 2347.

[30] A. Hammouche, E. Karden, R.W. De Doncker, J. Power Sources 127 (2004) 105.

[31] W.A. Adams, J. Power Sources, in press.

[32] M. Verbrugge, E. Tate, J. Power Sources 126 (2004) 236.

[33] Y. Cadirci, Y. Ozkazanc, J. Power Sources 129 (2004) 330.

[34] S.A. Ilangovan, Ph.D. Thesis, Indian Inst. Sci., Bangalore, 1991.

[35] S.A. Ilangovan, S. Sathyanarayana, J. Appl. Electrochem. 22 (1992) 456.

[36] C. Martinez, Y. Drori, J. Ciancio, XICOR Application Note, AN127, October 1999.